

Simulation Validation of Experimental Tests for Automotive System EMC Developmental Tests

Giacomo Braglia¹, Alistair Duffy², and Sami Barmada¹

¹Department of Energy, Systems, Territory and Construction Engineering
University of Pisa, 56122 Pisa, Italy
braglia.giacomo@gmail.com, sami.barmada@unipi.it

²School of Engineering and Sustainable Development
De Montfort University, Leicester, LE1 9BH, United Kingdom
apd@dmu.ac.uk

Abstract – The development and testing of automotive (sub)systems, particularly for Electromagnetic Compatibility (EMC), usually requires expensive test facilities. This paper describes the use of electromagnetic simulation to demonstrate the level of confidence that can be placed in measurements taken in more general laboratories, thus giving an estimate of the accuracy these facilities can provide. This is important in order to enable/allow more developments in automotive systems from research and development teams without standards compliant test facilities. This is, itself, important because of current developments in all-electric and autonomous vehicles. This paper demonstrates, through the use of full wave simulation representing a theoretically ideal environment compared with two different practical approaches, that EMC analysis can be undertaken with a reasonable estimation of accuracy and provides a framework for pre-compliance or developmental testing.

Index Terms – Automotive engineering, EMC, pre compliance tests, radiated emissions.

I. INTRODUCTION

The number and complexity of electric and electronic systems in modern automobiles has increased dramatically over recent years. The advent of the ‘driverless car’ is set to increase that further. As a consequence, electromagnetic compatibility (EMC) is of great concern from both an operational and safety viewpoint. In the automotive environment, the source of the radiated emissions are frequently the connecting cables rather than the devices that the cables connect. These cables may be electrically long and can radiate efficiently [1].

The International Standard dealing with automotive EMC is “CISPR 25” [2], which contains the limits and the procedures for the measurement of radio disturbances

for automotive components and subsystems as well as a complete vehicle. It recommends the use of Absorber-Lined Shielded Enclosures (ALSE) in radiated emissions measurements tests, most commonly this is a semi anechoic chamber.

Given that rectifying EMC problems becomes costlier the later they are discovered, there is clear benefit in the use of pre-compliance and developmental tests in order to reduce the costs [3] as well as testing during development. This paper is concerned with comparing measurements and simulation results to provide that confidence measure. Moreover, two approaches to obtain measured results are discussed by way of “triangulating” the conclusions. These are measurement of a full system and prediction of the full system behaviour based on elemental measurements. This paper is only concerned with common mode currents as these represent the most significant source of radiation.

Recently, reference [4] proposed a method, based on a Hertzian dipole model, to calculate the radiated emissions from a cable harness in vehicles. This method divided the common mode path into a set of short, elemental, segments and used the frequency domain measurements of common mode currents to calculate, by superposition, the overall resulting field. This method is called the *multi-dipole model*. The same authors, in [5], proposed an improvement to the multi-dipole model with measurements in the frequency domain. The advantage of this method is that they can obtain the radiated emission only from common mode currents and do not require the use of the semi-anechoic chamber: providing a test approach with greater utility for development teams without specialist resources.

Using similar logic, [6] presents a method (in accordance with CISPR 25) based on Multiple Segment Transfer Functions (MSTF). This method uses Transfer

Functions (TF) which represent the correlation between the common mode current in a specific setup environment and the radiated electric field strength.

The chief advantage of the MSTF method is that it helps to minimize the number of test cycles in the anechoic chamber. In fact, it allows the anechoic chamber to be used only once: in order to obtain the TF. Afterwards, the common mode current measurements can be taken for each component in any ordinary laboratory. Combining the last current measurements with the TF, previously obtained, the radiated electric field can be obtained.

Within this study, the MSTF method presented in [6], is replicated without using an anechoic facility. It approximates this by using an electromagnetically shielded room with a small number of radiation absorbing panels around the test system as a simple analogue of a semi anechoic chamber.

II. PRE-COMPLIANCE TEST METHOD FOR RADIATED EMISSION OF AUTOMOTIVE COMPONENT

The setup for radiated emission for components, presented in CISPR 25, comprises a line-over-ground-plane. The ground plane is a flat conductive surface whose potential is used as a common reference. The test harness is placed on a non-conductive material at 50 ± 5 mm above the ground plane.

The wiring type is defined by the actual system application and requirement. The length of the test harness is 1500 ± 75 mm and the antenna is positioned 1000 ± 10 mm from the wiring harness.

The test method relies on the common mode currents and the Transfer Functions to predict the electric field while differential mode currents are neglected due to the closely spaced geometry of the harness [7], [8]. In this work the harness used is a twisted pair cable. For convenience the line over ground plane, according to CISPR 25, is called *big line*.

Transfer functions (TFs) give the correlation, in the frequency domain, between the common mode currents along the harness and the radiated emissions. TFs are calculated with measurements made in the ALSE, thus the properties of the test setup are contained in the TFs.

The transfer function is defined by [1]:

$$TF(f) = \frac{E}{I_{CM}}, \quad (1)$$

where the I_{CM} is the common mode current along the cable harness and E is the electric field strength.

The TF can be obtained either by using an antenna connected to the test receiver and signal generator or by using measurements of the scattering parameters performed with a Vector Network Analyzer (VNA). The latter is the approach used in this work.

The line is fed by port 1 of the VNA and it is

terminated with a load to simulate the equipment under test (EUT).

The measurements can be performed in two steps. Figure 1 shows the setup block diagram of the first step, where the scattering parameters ($S_{21_antenna}$) is measured with the VNA. To measure the $S_{21_antenna}$ the line is fed by port 1 of the VNA and the port 2 is connected to the antenna.

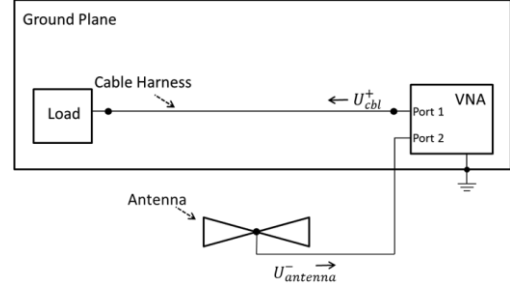


Fig. 1. Setup block diagram for $S_{21_antenna}$, to obtain TF.

In the second step port 1 of VNA feeds the line, whilst port 2 is connected to the current probe, which is located around the cable. In this step the scattering parameter (S_{21_CP}) is measured. This is illustrated in Fig. 2.

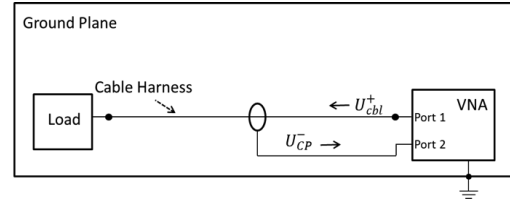


Fig. 2. Setup block diagram for S_{21_CP} , to obtain TF.

The transfer function can be calculated by Equation (2) [8]:

$$TF(f) = \left| \frac{S_{21_antenna}(f)}{S_{21_CP}(f)} \right| AF(f) Z_T(f), \quad (2)$$

where:

- AF is the antenna factor.
- Z_T is the transfer impedance of the current probe.

III. MULTIPLE SEGMENTS TRANSFER FUNCTIONS (MSTF)

The method presented in [8] considers the cable harness of the EUT as single segment, thus uses only one current probe measurement of the common mode currents. This method is limited, because it needs an identical current distribution of the EUT setup and the TF generation setup [3].

The MSTF approach divides the cable harness representing the radiation source in segments, for each of them the contribution of electric field is calculated. To

obtain the predicted electric field, a union of the contributions for each segment is made taking into account the phase due to the different distance of each segment from the antenna.

A. Small line segmentation

The segmentation of the line is made by building a *small line* with the same type of the cable harness.

The length of the *small line* should be electrically small compared to the wavelength of the upper limit of the frequency range. This ensures a constant current distribution along the segment. Figure 3 shows the electrical scheme of the line.

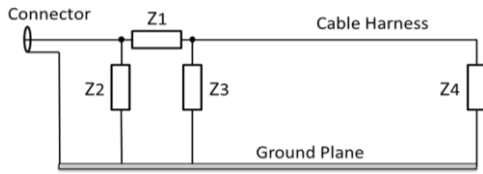


Fig. 3. Electrical scheme of the *small line*.

The line is terminated with an impedance (Z_4) whose value is as close as possible to the characteristic impedance of the line and at the near end a network of impedances with π scheme is connected in order to provide an impedance match.

B. TF in the MSTF

For each *small line* the TFs are calculated according to Equation (2). S-parameter measurements, needed to calculate the TF, have to be made in the ALSE according to CISPR 25.

$S_{21_antenna}$ needs to be measured using the *small line* positioned on the ground plane of the *big line* (see Fig. 4): port 1 feeds the *small line* and port 2 is connected to the antenna.

To measure S_{21_CP} the current probe is positioned around the wire in the middle of the *small line*. The VNA is used connecting port 1 to the *small line* and port 2 to the current probe.

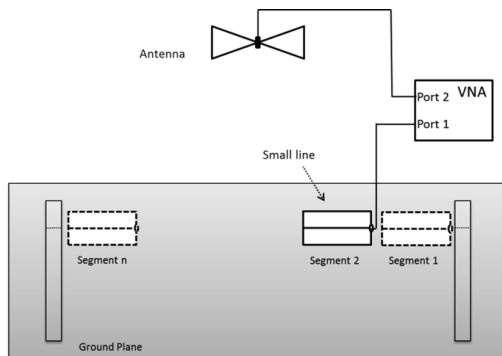


Fig. 4. Measurement setup for $S_{21_antenna}$.

C. Common mode current determination

The knowledge of the common mode current distribution along the cable is needed for the radiated emission calculation.

The distribution of common mode current can be obtained through measurements of the current envelopes. Those measurements are made along the cable with the current probe and a test receiver in peak mode, illustrated in Fig. 5.

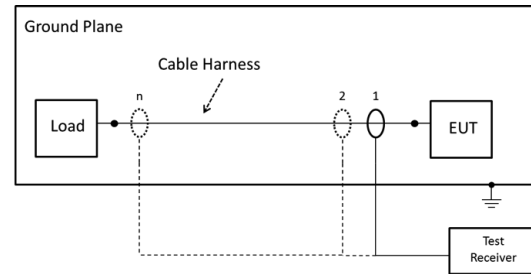


Fig. 5. Measurement setup for common mode current envelopes.

The current distribution from the envelope measurements can be obtained from a cable that is (ideally) longer than half the wavelength of frequency of test. However, for a shorter cable length, it is still an appropriate approximation and the procedure is the one reported in [6].

D. Phase determination

In the MSTF method, phase shift information between the segments is needed. This can be obtained with the current probe measurements along the cable of the EUT test setup. The measurements have to be made in the same positions where the TFs are generated. Using the VNA, the *big line* is fed at port 1 and port 2 is connected to current probe, see Fig. 6.

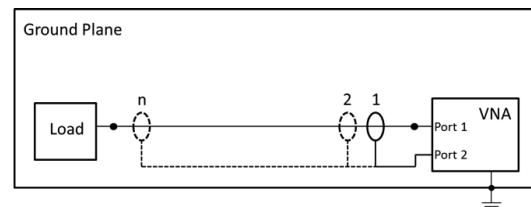


Fig. 6. Measurements of currents phase shifts, with current probe.

The phase shift is equivalent to the angle of S_{21} , see Equation (3):

$$\varphi_{1,i}(f) = \angle S_{21,i}. \quad (3)$$

Each segment has different distance r_i from the antenna. This causes phase shift of the electric field $\varphi_{E,i}(f)$.

As shown in Equation (4), $\varphi_{E,i}(f)$ is equivalent to the angle of $S_{21_antenna}$ parameter, which is measured using the *small line* and the antenna, see Fig. 4:

$$\varphi_{E,i}(f) = \angle S_{21_antenna,i} \quad (4)$$

D. Prediction of the electric field

The calculation of the electric field can be performed with the previous information of each segment. As can be seen in the Equation (5), the electric field is given by superposition of each segment's field:

$$E_{pred}(f) = \left| \sum_i TF_i(f,y) I_{EUT,i}(f) e^{j[\varphi_{T,i}(f) + \varphi_{E,i}(f)]} \right| \quad (5)$$

IV. MEASUREMENTS

The measurements are divided in two parts: one is dedicated to the implementation of the MSTF as described in the previous sections (measurements on the *small line* and of common mode currents) while the second part simply consists of a direct measurement of the E field produced by the *big line*.

The cable was a common twisted pair technology (category 5E cable). The diameter of each wire was 0.51 mm and the length of the line was 1.5 m. Measurements were made with the VNA in a screened room with a number of RAM panels used to provide a crude analogue of the ALSE.

The frequency range of the measurements was 30 to 200 MHz, representing a compromise between the emissions spectrum and acceptable dynamic range of the measurement systems. However, it should be noted that the system noise floor was high below 60 MHz so results at these frequencies are not to be regarded as reliable but they are included here to provide a fuller representation of the experimental results for validation by simulation.

Measurements on the *small line* are performed to calculate S_{21_CP} and $S_{21_antenna}$ as previously described; Fig. 7 shows the current probe around the *small line*'s cable.

As for the common mode currents, the setup was made with the VNA, acting as a broadband source, which fed the *big line* that was terminated with a 50 Ω Load. The currents were measured with the current probe around the *big line*'s cable and connected to the spectrum analyser configured as a peak detector.

In the second part a radiated emission measurements serving as reference to validate the E- field predictions were made. These were made using the same setup used in the common mode measurements, but the current probe was taken off and the spectrum analyser was connected to the antenna. Measurements in the range of 1 MHz to 200 MHz were made to see how the noise floor could affect the tests at the low frequencies.

The measurement, with antenna and spectrum analyzer, was made while the line was fed from the

VNA. Then, the measurement was made with the line disconnected, but leaving the VNA turned on inside the chamber.

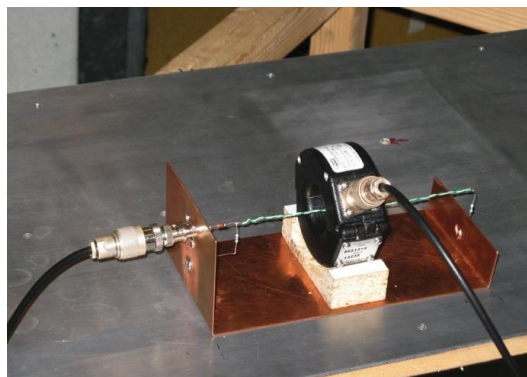


Fig. 7. Measurements with *small line* and current probe.

V. SIMULATION

Computer Simulation Technology CST Studio Suite (CST) was used to generate the reference data used to evaluate the measurements. The measurement systems were replicated as closely as possible. However, ideal free space characteristics were used. This was to allow the representation of what could be expected from the measurements if they were to be undertaken in a theoretically ideal facility. It was previously noted that only the common mode currents were to be considered, so it would have been possible to represent the Category 5 twisted pair with a single conductor in the model (which would have been computationally simpler). However, it was decided to replicate the EUTs as closely as possible so a twisted pair, of the correct dimensions and lay length was created, as illustrated in Fig. 8.

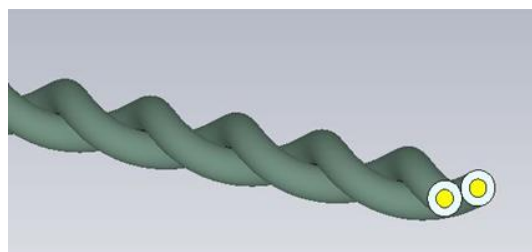


Fig. 8. Model of the twisted pair.

This cable was terminated in the test fixture using a coaxial connector. The simulated version of this is shown in Fig. 9.

The overall simulation configuration is illustrated in Fig. 10, which shows the line being simulated and the E-field probe location, which provides further 'idealised' measurements by removing the effect of the measuring antenna on the results.

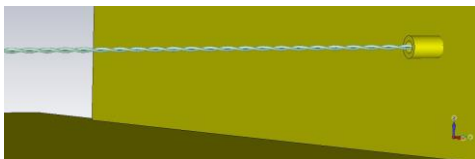


Fig. 9. Termination of the twisted pair.

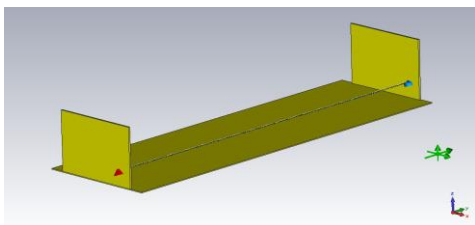


Fig. 10. Simulation configuration.

VI. POST PROCESSING AND RESULTS

This section presents the measurement results, showing how the electric field can be retrieved from the common mode currents and these are compared with the simulations.

The measurements were performed using the biconical antenna and the spectrum analyser. Using the antenna factor, the E field was retrieved in vertical and horizontal polarization. Remembering that the equipment was in the chamber during the tests, Fig. 11 shows how the noise floor could affect the measurements in low frequency.

Figures 12 and 13 show the comparisons between the electromagnetic simulations, the measured E field and the predicted E field, both in the horizontal polarization (Y) and in the vertical polarization (Z).

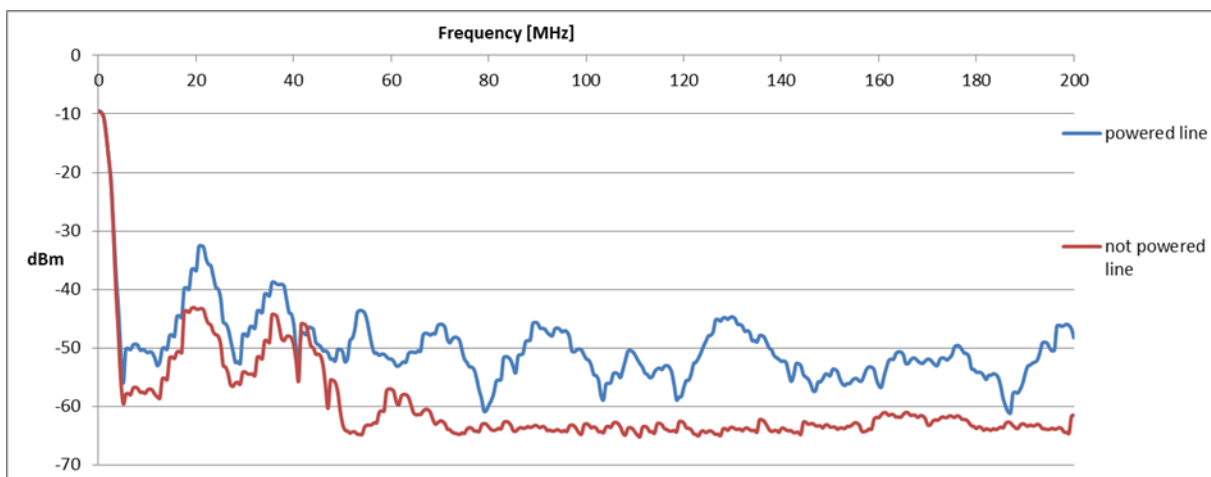


Fig. 11. Comparison, between the measurements with the big line powered and the big line not powered, to see how the noise floor affects the measurements in low frequency.

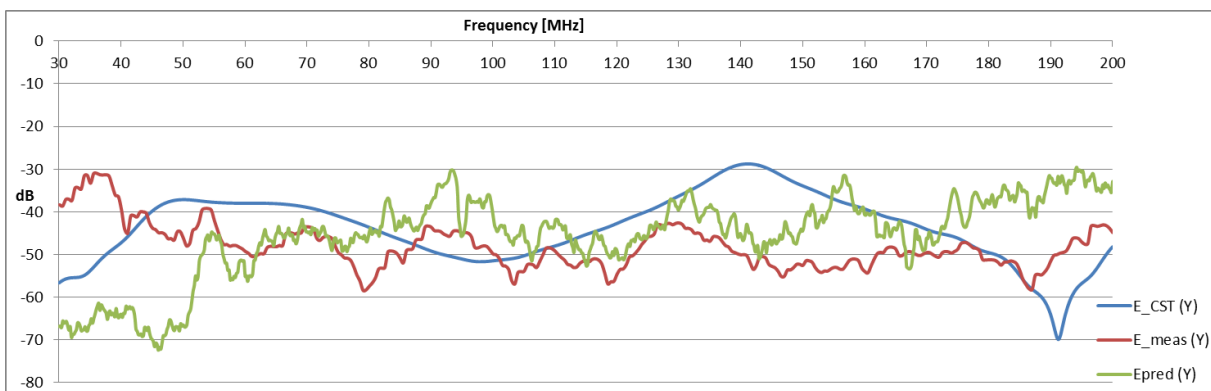


Fig. 12. Comparison for horizontal polarization (Y) of the predicted E field, measured E field and E field CST simulated.

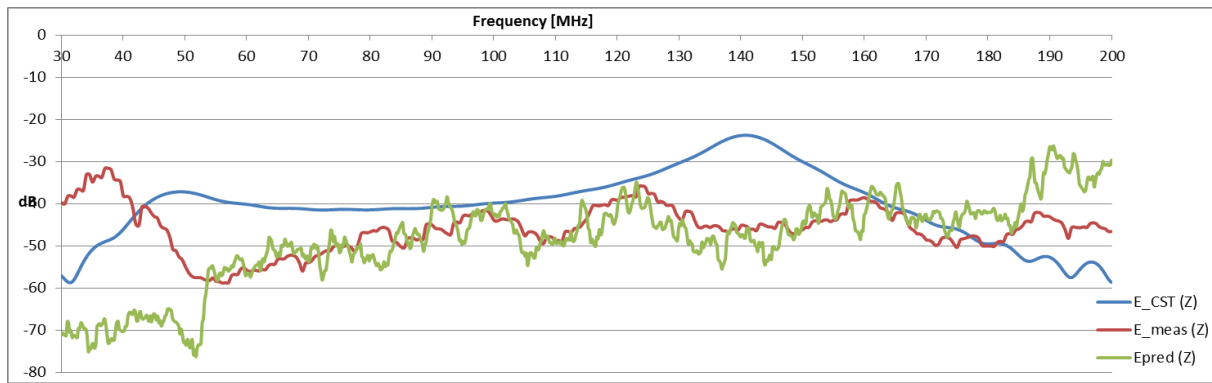


Fig. 13. Comparison for vertical polarization (Z) of the predicted E field, the measured E field and the simulated E field in CST.

At low frequencies (up to 60 MHz) a large difference between the measured E-field and the predicted E field can be seen, the cause of this difference is likely to be the noise floor, because the absorbent materials do not work well at those lower frequencies.

The CST simulations traces are close to the predicted and measured field with an average deviation lower than 10 dB in the most of the frequency range. It is important to underline that in CST the chamber environment is not considered (metal walls, absorbing materials and antenna) and is, therefore, an 'ideal' configuration: this explains the big differences between the blue curves (CST) and the red/green curves in some frequency bands.

In the horizontal polarization (Fig. 12) above 50 MHz the predicted E-field and the measured E-field are in good agreement. In the frequency ranges 150 to 160 MHz and 180 to 200 MHz a difference of about 10 dB can be seen.

In the vertical polarization (Fig. 13) above 50 MHz, the predicted E-field and the measured E-field are in good agreement. Only in the frequency range 190 to 200 MHz the difference is about 10 dB.

The comparison has to be made taking into account that an approximation of a semi anechoic chamber was used. Therefore the absorbent materials were located around the setup but they did not cover all walls. Also the measurement equipment was located in the chamber, thus the equipment supply could produce signals that affect the measurements. This was to investigate how well a low cost general laboratory configuration would behave.

Furthermore, in the test configuration, the antenna is in the near field of the line, while the antenna factor from manufacturers is calibrated in far field in an open area test site [9]. This is likely to have an affect the prediction of electric field.

VI. CONCLUSION

One of the principal interests of this paper has been

to identify how accurate radiation emissions measurements can be if they are performed in a general laboratory setting. An important aspect of this work has been the use of 3-D full-wave simulations to validate the measurements

The simulations show general agreement with the experiments, giving an indication of the deviation that can be expected from a theoretically ideal configuration. There is clearly some difference in the fine detail, but the general shapes and amplitudes demonstrate reasonable overall agreement.

This work shows that with good measurement practice, a possible test methodology is suitable to be used by a range of interested parties: from automotive components manufacturers to academic teaching and research laboratories can be obtained. This proposed methodology can give results with an accuracy of few dB. It also shows the benefit of the use of simulation to validate measurements. In the case of the results presented here, a shielded room was used. However, it may be possible to use a less isolated environment provided that the initial 'site survey' identifies the noise floor characteristics (as was shown in Fig. 9) and results are not relied on where the noise floor (including background radiation) is too high.

ACKNOWLEDGMENT

The authors would like to acknowledge the support of the EU Erasmus scheme that allowed this work to be undertaken.

REFERENCES

- [1] W. T. Smith and R. K. Frazier, "Prediction of anechoic chamber radiated emissions measurements through use of empirically-derived transfer functions and laboratory common-mode current measurements," *Electromagnetic Compatibility, 1998. 1998 IEEE International Symposium on*, vol. 1, pp. 387-392, August 1998.
- [2] British Standards Institute, "Radio disturbance

characteristics for the protection of receivers used on board vehicles, boats, and on devices - Limits and methods of measurement,” BS EN 55025:2003 CISPR 25:2002, March 2003.

- [3] D. Schneider, M. Bottcher, S. Tenbohlen, and W. Kohler, “Pre-compliance test method for radiated emissions with multiple segment transfer functions,” *International Symposium on Electromagnetic Compatibility (EMC EUROPE 2013)*, pp. 605-610, August 2013.
- [4] J. Jia, D. Rinas, and S. Frei, “Prediction of radiated fields from cable bundles based on current distribution measurements,” *International Symposium on Electromagnetic Compatibility (EMC EUROPE 2012)*, pp. 1-7, September 2012.
- [5] J. Jia, D. Rinas, and S. Frei, “An alternative method for measurement of radiated emissions according to CISPR 25,” *International Symposium on Electromagnetic Compatibility (EMC EUROPE 2013)*, pp. 304-309, September 2013.
- [6] D. Schneider, et al., “Transfer functions and current distribution algorithm for the calculation of radiated emissions of automotive components,” *International Symposium on Electromagnetic Compatibility (EMC EUROPE 2013)*, pp. 443-448, September 2013.
- [7] Clayton R. Paul, “A comparison of the contributions of common-mode and differential-mode currents in radiated emissions,” *Electromagnetic Compatibility, IEEE Transactions on*, vol. 31, no. 2, pp. 189-193, May 1989.
- [8] D. Schneider, S. Tenbohlen, and W. Kohler, “Pre-compliance test method for radiated emissions of automotive components using scattering parameter transfer functions,” *International Symposium on Electromagnetic Compatibility (EMC EUROPE 2012)*, pp. 1-6, September 2012.
- [9] D. Rinas, J. Jia, A. Zeichner, and S. Frei, “Substituting EMC emission measurement by field and cable scan method using measured transfer function,” *Advances in Radio Science*, vol. 11, pp. 183-188, July 2013.



Giacomo Braglia received the M.S. degree in Electrical Engineering at the University of Pisa in year 2014 and he received the Rohde & Shwartz Prize for Best Project for his Master’s thesis. He is currently Project Quality Manager on for GE Oil & Gas (SubSea systems).



Alistair Duffy is Professor of Electromagnetics at De Montfort University, Leicester, UK, having joined from the University of Nottingham in 1994 where he obtained his Ph.D. in 1993. He holds a Bachelors and Masters degree from the University of Wales (University College Cardiff) and an MBA from the Open University. He is a Fellow of the IEEE and a past Board of Directors member of both the Applied Computational Electromagnetics Society and the IEEE EMC Society. His research interests are in computational and experimental electromagnetics, particularly focusing on EMC and validation problems.



Sami Barmada received the M.S. and Ph.D. degrees in Electrical Engineering from the University of Pisa, Italy, in 1995 and 2001, respectively. He currently is an Associate Professor with the Department of Energy and System Engineering (DESTEC), University of Pisa. His teaching activity is related to circuit theory and electromagnetics. His research activity is mainly dedicated to numerical computation of electromagnetic fields and EMC problems, power line communications, non-destructive testing and signal processing. He is author and co-author of approximately 100 papers in international journals and refereed conferences. Barmada was the General Chair of the ACES 2007 Conference and Technical Chairman of the PIERS 2004 ACES 2013 and ACES 2014 conferences. He is currently President of the ACES Society.